(b) For angles $\theta > \pi/2$ the cross section does not vary as rapidly, and at the limit $\theta \approx \pi$ it has the value $d\sigma/d\Omega = k = 1.2 \times 10^{-24}\ \text{cm}^2$. Precise measurements at these large angles reveal deviations from the Rutherford equation and are due to the strong interaction (nuclear interaction, see Table 6.1) between the alpha particle and the gold nucleus.

As explained in detail in the introduction to this chapter, the nuclear interaction will manifest itself only at short distances—that is, at high-momentum transfers q (Eq. 1.4), where $q = 2p \sin \theta/2$. Clearly the maximum momentum transfer in this experiment is

$$q = 2p = 2\sqrt{2Em} = 200\ \text{MeV}/c$$

The recent experiments on Coulomb scattering of electrons from protons have been extended to $q \simeq 2.2$ BeV/c.

3. Compton Scattering

3.1 Frequency Shift and Cross Section

This section deals with the scattering of electromagnetic radiation by free electrons. As mentioned in the introduction to this chapter, it is the scattering of electromagnetic radiation from various objects that makes it possible for us to "see" them. However, as the frequency of the radiation is increased beyond the visible region, the light quanta have energies comparable to, or larger than the binding energy of the electrons in atoms, and the electrons can therefore be considered as free.

In 1920 A. H. Compton investigated the scattering of monochromatic x-rays from various materials. He observed that after the scattering, the energy (frequency) of the x-rays had changed, and had always decreased. From the point of view of classical electromagnetic theory, this frequency shift cannot be explained,† since the frequency is a property of the incoming electromagnetic wave (field) and cannot be altered by the change of direction implied by the scattering. If, on the other hand, we think of the incoming radiation as being represented by a beam of photons, we need only consider the scattering of a quantum of energy $E = h\nu$ from a free electron; then, because of energy-momentum conservation, the scattered quantum has energy $E' = h\nu' < E$, in complete agreement with the experiments of Compton.

The frequency shift will depend on the angle of scattering and can be easily calculated from the kinematics. Consider an incoming photon of energy $E = h\nu$ and momentum $p = h\nu/c$ (Fig. 6.8) scattering from an electron of mass m; $\mathbf{p}$ is the momentum of the electron after scattering and

† See, for example, J. D. Jackson, *Classical Electrodynamics*, John Wiley, p. 488.

Fig. 6.8 Compton scattering of a photon from a free electron.

$h\nu'$, $\mathbf{h}\nu'/c$ the energy and momentum of the photon after the scattering. The three vectors $\mathbf{h}\nu/c$, $\mathbf{h}\nu'/c$, and $\mathbf{p}$ must lie on the same plane, and energy conservation yields

$$h\nu + mc^2 = h\nu' + \sqrt{p^2c^2 + m^2c^4} \tag{3.1}$$

From momentum conservation we obtain

$$h\nu = h\nu' \cos\theta + cp \cos\phi \tag{3.2}$$

$$0 = h\nu' \sin\theta + cp \sin\phi \tag{3.3}$$

Here θ is the photon scattering angle, and ϕ the electron recoil angle. To solve the above equations we transpose appropriately, square, and add Eq. 3.2 and Eq. 3.3 to obtain

$$h^2\nu^2 - 2h^2\nu\nu' \cos\theta + h^2\nu'^2 = c^2p^2$$

while by squaring Eq. 3.1,

$$h^2\nu^2 + h^2\nu'^2 - 2h^2\nu\nu' + 2hmc^2(\nu - \nu') = c^2p^2$$

which by subtraction yields

$$\frac{\nu - \nu'}{\nu\nu'} = \frac{h}{mc^2}(1 - \cos\theta) \tag{3.4}$$

We can recast Eq. 3.4 into two more familiar forms: (a) to give the shift in wavelength of the scattered x-ray beam:

$$\Delta\lambda = \lambda' - \lambda = \frac{h}{mc}(1 - \cos\theta) \tag{3.5}$$

or (b) to give the energy of the scattered photon:

$$E' = \frac{E}{1 + (E/mc^2)(1 - \cos\theta)} \tag{3.6}$$

From Eq. 3.5 we see that the shift in wavelength, except for the angular dependence, is a constant, the Compton wavelength†

$$h/mc = 2.42 \times 10^{-10}\ \text{cm} = 0.0242\ \text{Å}$$

For low-energy photons, with $\lambda \gg 0.02$ Å, the Compton shift is very small, whereas for high-energy photons with $\lambda \ll 0.02$ Å, the wavelength of the *scattered* radiation is always of the order of 0.02 Å, the Compton wavelength. These conclusions can equally well be obtained from Eq. 3.6, where the energy shift increases when E/mc^2 becomes large. For $E/mc^2 \gg 1$, E' is independent of E and of the order $E' \approx mc^2$. [Hence $\lambda' = c/\nu' = c/(E'/h) \simeq c/(mc^2/h) = h/mc$ as stated before.]

As an example, in this laboratory gamma rays from Cs^{137} are scattered from an aluminum target; since $E = 0.662$ MeV, we have $E/mc^2 = 1.29$, so that back-scattered gamma rays ($\theta = 180°$) will have $E' = E/3.6$, which is less than 30 percent of their original energy. It thus becomes quite easy to observe the Compton energy shift as compared to x-ray scattering, where, if we assume $\lambda = 2$ Å, $\Delta\lambda/\lambda = \Delta E/E = 0.01$.

In the original experiments Compton and his collaborators observed (especially for high Z materials) in addition to the frequency shifted x-rays, scattered radiation *not shifted* in frequency. The unshifted x-rays are due to scattering from electrons that remained bound in the atom‡: in this process the recoiling *system* is the entire atom, and we replace in Eq. 3.5 m by m_A (where $m_A \simeq 2{,}000 \times A \times m_e$) resulting in an undetectable wavelength shift, $\Delta\lambda' \simeq 10^{-7}$ Å.

Next we are interested in the differential cross section for the scattering of the radiation from the electrons. Classically this is given by the Thomson cross section,§ which can be easily derived: consider a plane wave propagating in the z direction with the E vector linearly polarized along the x direction. This is incident on an electron of mass m, as shown in Fig. 6.9 The electron will experience a force $F = eE = eE_0 \cos \omega t$, and its acceleration will be

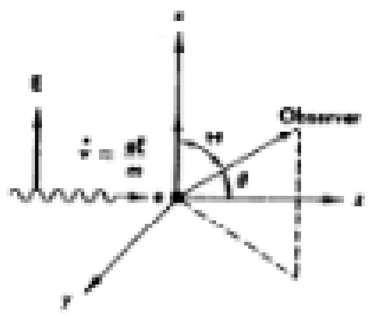

FIG. 6.9 Classical picture of the scattering of electromagnetic radiation by an electron; this leads to the Thomson cross section.

$$\ddot{x} = \frac{eE_0}{m} \cos \omega t$$

† The mass of the electron m_e was used in evaluating h/mc; by using the mass of the pion, or other particle, we obtain the pion Compton wavelength, and so forth.

‡ A similar situation is discussed in the following section on the Mössbauer effect, where the nucleus remains bound in the lattice and the recoiling system is the entire crystal.

§ Already discussed in Chapter 5, Section 2.5.

According to Eq. 2.26, Chapter 5, the power radiated by this accelerated electron will be (nonrelativistically, in MKS units)

$$\frac{dP}{d\Omega} = \frac{e^2}{(4\pi\epsilon_0)^2 \mu_0 c^3}\, \ddot{x}^2 \sin^2 \Theta \tag{3.7}$$

where Θ is the angle between the direction of observation and the E vector of the incoming wave. Using the expression for $\ddot{x}$, we can write for Eq. 3.7 averaged over one cycle

$$\left\langle \frac{dP}{d\Omega} \right\rangle = \frac{1}{2} \left(\frac{e^2}{4\pi\epsilon_0 mc^2} \right)^2 \epsilon_0 E_0^2 c \sin^2 \Theta$$

Finally, from the definition for a cross section given in Chapter 5, Section 2.1, we have

$$\frac{d\sigma}{d\Omega} = \frac{\text{energy radiated/(unit time-unit solid angle)}}{\text{incident energy/(unit area-unit time)}}$$

Here the denominator is clearly given by the Poynting vector

$$\langle P \rangle = \frac{1}{2} \sqrt{\frac{\epsilon_0}{\mu_0}}\, E_0^2 = \tfrac{1}{2} \epsilon_0 c E_0^2$$

Thus we obtain

$$\frac{d\sigma}{d\Omega} = \left(\frac{e^2}{4\pi\epsilon_0 mc^2} \right)^2 \sin^2 \Theta \tag{3.8}$$

Where

$$\frac{e^2}{4\pi\epsilon_0 mc^2} = r_0$$

has dimensions of length, the so-called "classical electron radius"

$$r_0 = 2.82 \times 10^{-13}\ \text{cm}$$

Finally, we average over all possible directions of polarization of the incoming wave and use the angle θ measured from the direction of propagation of the wave to obtain

$$\frac{d\sigma}{d\Omega} = r_0^2 \left(\frac{1 + \cos^2 \theta}{2} \right) \text{cm}^2 \tag{3.9}$$

When integrated over all angles, Eq. 3.9 yields the Thomson cross section

$$\sigma_T = \frac{8\pi}{3} r_0^2 \tag{3.10}$$

(also given in Chapter 5, Eq. 2.19).

Several objections can be raised to the simple cross section given by Eq. 3.9 or Eq. 3.10: (a) it does not depend on frequency, a fact not supported by experiment; (b) the electron, even though free, is assumed not to recoil; (c) the treatment is nonrelativistic; and (d) quantum effects are not taken into account. Indeed, the correct quantum-mechanical calculation for Compton scattering yields the so called Klein-Nishina formula†

$$\frac{d\sigma}{d\Omega} = r_0^2 \frac{1 + \cos^2\theta}{2} \frac{1}{[1 + \gamma(1 - \cos\theta)]^2} \times \left[1 + \frac{\gamma^2(1 - \cos\theta)^2}{(1 + \cos^2\theta)[1 + \gamma(1 - \cos\theta)]}\right] \quad (3.11)$$

where r_0 and θ were defined previously, and $\gamma = h\nu/mc^2$. The cross section has been averaged over all incoming polarizations. By integrating Eq. 3.11, the total cross section can be had. We will not give the complete result here, but the asymptotic expressions have already been presented in Chapter 5, Eq. 2.21.

A comparison of the Thomson (Eq. 3.9) and Klein-Nishina cross sections, including the results obtained in this laboratory for $\gamma = 1.29$, is shown in Fig. 6.14. We remark that although the Thomson cross section is symmetric about 90°, the Klein-Nishina cross section is peaked forward strongly as γ increases. This is due to a great extent to kinematical factors associated with the Lorentz transformation from the center of mass to the laboratory; note that the center of mass velocity of the (quantum + free electron) system is

$$v = \beta c = c\gamma/(1 + \gamma)$$

where as before $\gamma = h\nu/mc^2$.

The experimental data are in perfect agreement with the results of Eqs. 3.6 and 3.11, which are among the most impressive and convincing successes of quantum theory. In the following two sections we will describe the experimental verification of these predictions.

3.2 The Compton Scattering Experiment

As with any scattering experiment, the apparatus will consist of:

(a) The beam of incident particles, in this case photons.
(b) The target (containing the electrons from which the photons scatter).
(c) The detector of the scattered photons.

† See W. Heitler, *The Quantum Theory of Radiation*, 3rd ed., Oxford University Press, p. 219.

The beam of photons is obtained by collimating the gamma radiation from a Cs^{137} source. As we know (Table 4.2) Cs^{137} (Ba^{137}) emits a gamma ray of energy 0.662 MeV, and the detection techniques have been discussed in Chapter 5. In Fig. 5.28 is shown the pulse-height spectrum of the gamma radiation from Cs^{137}, as obtained with standard equipment; the same detection equipment is used in this experiment with the only difference that the scintillation crystal is placed in a heavy shield.

A schematic of the apparatus is shown in Fig. 6.10. The lead pig *A* is fixed and holds the source, which can be introduced through the vertical hole (v). Another lead shield *B* contains the detector and can be rotated about the center, where the target is located. The lead assemblies are rather heavy (approximately 200 lb) and some provisions must be taken for adequate mounting.

For the source, a 35-mCi Cs^{137} sample was used, which was properly encapsulated before being shipped to the laboratory. It should always be transported in a lead container, and when transferred into the lead pig *A*, it must be handled only by the attached string. The source holder (*A*) has a collimator (*h*) drilled horizontally, subtending a solid angle of the order of 0.03 sr. Of interest to us will be the density of the photon beam at the target, and the *expected* value is

$$\frac{3.7 \times 10^{10} \times 0.035}{4\pi} \frac{1}{r^2} = 8.8 \times 10^4 \text{ photons/cm}^2\text{-sec}$$

Where we use $r = (13.5 \times 2.54) = 34.3$ cm, as read off Fig. 6.10; indeed the observed density of 41×10^4 photon/cm²-sec is of the predicted order of magnitude.

In contrast to the situation in Rutherford scattering, there is no need to enclose the beam and detector in vacuum or to use a very thin target. We know that gamma rays do not gradually lose energy when traversing matter as a charged particle does, but their interaction can be characterized by a mean free path. For the Cs^{137} gamma ray we find from Fig. 5.34

$$\lambda = 4.7 \text{ cm in Al}; \qquad \lambda = 0.92 \text{ in Pb}$$

this corresponds to 10^4 cm of air, so that the interaction of the photon beam in the air of the apparatus (approximately 100 cm) is indeed negligible. Also, the target thickness can safely be a fraction of a mean free path before the probability for multiple interactions becomes considerable. Aluminum targets ½-in. thick are quite adequate for this experiment.

Some special mention must be made of the geometrical shape of the target. We may use a flat target (such as an aluminum plate), in which event the cross section is obtained by considering the interaction of the total beam with the number of electrons per square centimeter of the